Journal of Hydrology: Regional Studies 19 (2018) 318–334

Contents lists available at ScienceDirect

Journal of Hydrology: Regional Studies

journal homepage: www.elsevier.com/locate/ejrh

A conceptual study of offshore fresh groundwater behaviour in the Perth Basin (Australia): Modern salinity trends in a prehistoric context

Leanne K. Morgan[a,b,*], Adrian D. Werner[b,c], Aine E. Patterson[d]

[a] Waterways Centre for Freshwater Management, University of Canterbury, Private Bag 4800, Christchurch 8140, New Zealand
[b] College of Science and Engineering, Flinders University, GPO Box 2100, Adelaide, SA 5001, Australia
[c] National Centre for Groundwater Research & Training, Flinders University, GPO Box 2100, Adelaide, SA 5001, Australia
[d] Department of Water and Environmental Regulation, The Atrium, Level 4, 168 St Georges Terrace, Perth, WA 6000, Australia

ARTICLE INFO

Keywords:
Offshore freshwater
Subsea aquifers
Groundwater
Seawater intrusion
Perth Basin

ABSTRACT

Study region: Fresh groundwater is thought to occur off the coast of Perth, Western Australia, in the confined Leederville and Yarragadee aquifers. Onshore hydraulic heads suggest that offshore groundwater may be augmenting onshore groundwater extraction, which is a critical component of Perth's water supply.

Study focus: To assess offshore freshwater conditions, we apply variable-density flow and transport modelling to a simplified cross-sectional representation of the Perth Basin offshore aquifers, developed using available hydrogeological information.

New hydrological insights for the region: Simulations suggest Perth's offshore fresh groundwater was emplaced during glacial periods (when sea levels were up to 120 m lower than today), and the interface between seawater and freshwater is likely still moving landward in response to paleo-conditions, albeit slowly (i.e., a maximum rate of 0.74 m/y was predicted). Onshore groundwater extraction is predicted to have increased the rate of inland interface movement by up to 75%, compared to the rate under paleo-conditions alone. Simulations including the offshore Badaminna Fault suggest that this feature truncates the offshore extent of fresh groundwater and reduces the rate of inland interface movement. The results of this investigation demonstrate that paleo-stresses may impose stronger controls than modern, human-induced factors on offshore freshwater extent in the Perth Basin, and that offshore faults may play a critical role in controlling offshore freshwater extent.

1. Introduction

Coastal groundwater investigations are traditionally based on the availability of freshwater in aquifers landward of the shoreline. However, Post et al. (2013) identified that vast offshore reserves of fresh groundwater occur within submerged fringes of continents globally. Offshore freshwater reserves can form via present-day terrestrial recharge to confined offshore aquifers that outcrop on land (Kooi and Groen, 2001; Bakker, 2006). Offshore groundwater may also be paleo-groundwater emplaced during the last or perhaps

* Corresponding author at: Waterways Centre for Freshwater Management, University of Canterbury, Private Bag 4800, Christchurch 8140, New Zealand.
E-mail addresses: leanne.morgan@canterbury.ac.nz (L.K. Morgan), adrian.werner@flinders.edu.au (A.D. Werner), aine.patterson@dwer.wa.gov.au (A.E. Patterson).

https://doi.org/10.1016/j.ejrh.2018.10.002
Received 13 August 2018; Received in revised form 11 September 2018; Accepted 14 October 2018

multiple glacial periods, when sea levels were significantly lower. Continental shelves were exposed to infiltration from rainfall, paleo-river systems and ice sheets in some cases (Meisler et al., 1984; Faure et al., 2002; Person et al., 2003), leading to trapped freshwater beneath the sea floor as sea levels rose to current levels.

The review of offshore freshwater by Post et al. (2013) highlights the paucity of data regarding subsea aquifers and the need to apply multiple methods to gain an improved understanding of key field sites. A common approach to the analysis of fresh groundwater resources is the application of numerical models. Prior studies of offshore freshwater that adopt computer modelling to study the evolution of paleo-conditions include Meisler et al. (1984) who used a cross-sectional steady-state model to estimate the sharp freshwater-saltwater interface position off the north Atlantic coast (near New Jersey, USA). They found that the current day measured interface position likely reflects a long-term average sea level of between 15 and 30 m below present-day conditions. Cohen et al. (2010) and Siegel et al. (2014) developed three-dimensional models for sections of the north Atlantic continental shelf and simulated both ice sheets and sea-level variations over periods of up to 3 million years before present (bp). Both studies found that ice sheet loading and sea-level low stands played important roles in the emplacement of offshore fresh groundwater in the region. Distal offshore freshwater was primarily the result of sea-level variation, whereas proximal freshwater was most strongly influenced by increased recharge beneath ice sheets at high latitudes. Amir et al. (2013) carried out two-dimensional modelling of offshore aquifers on the Mediterranean coast of Israel, in the Palmahim region. Steady-state and transient modelling (from 15 ky bp) that accounted for sea-level variations showed that the presence of a confining layer between upper and lower aquifers is necessary for offshore fresh groundwater to occur in this region. Recently, Michael et al. (2016) used steady-state numerical modelling of the Lower Bengal Delta aquifer system to show that geological heterogeneity can produce spatially complex subsurface salinity distributions that extend tens of kilometres offshore, even at steady state. There is little evidence of other attempts to numerically simulate subsea groundwater evolution.

Analytic steady-state sharp-interface solutions for the offshore extent of fresh groundwater have been developed by Kooi and Groen (2001), Bakker (2006), Bakker et al. (2017) and Werner and Robinson (2018). These solutions indicate that offshore fresh groundwater is most likely to occur within thick, highly permeable offshore aquifers that have a low-conductance overlying layer separating the aquifer from the ocean, and a high head at the coast. Applications of these analytic solutions by Kooi and Groen (2001) and Bakker (2006) to locations where offshore groundwater is thought to result from present-day terrestrial recharge (i.e., Hawaii at southern Oahu and the south Atlantic coast at Florida) indicated reasonable matches between the modelled and measured offshore freshwater extents. However, these analytical models cannot be applied within stacked aquifer systems, such as those that occur in the Perth region.

Fresh groundwater that is connected to onshore aquifers is thought to occur off the coast of Perth, Australia, although the volume and lateral extent of these resources are poorly characterised (Hennig and Otto, 2005; MWH, 2011; de Silva et al., 2013). Aquifers underlying Perth are important water sources for urban water supply and agricultural industries. For example, in 2008, groundwater comprised close to 100% (370 GL/year) of private water supply (i.e., from backyard and farm bores) and around 46% (of 286 GL/year) of reticulated public water supplies (Water Corporation, 2009, 2016; Department of Water, 2016a). The present study aims to improve the conceptual understanding of Perth's offshore fresh groundwater, in response to Post et al.'s (2013) call for greater knowledge of subsea aquifer conditions, particularly where onshore groundwater use may derive at least partly from offshore reserves. The study has significant implications for the Perth water supply, given that offshore freshwater may already be contributing to onshore groundwater extraction, as indicated by the preliminary assessment of Morgan and Werner (2015). Perth's offshore aquifers are investigated using variable-density flow and transport modelling applied to a simplified cross-sectional stratigraphic representation of the known hydrogeology, which was developed using information from offshore petroleum well logs, seismic data and onshore hydrogeology. The objectives of this study are to:

1) Explore whether Perth's offshore fresh groundwater was emplaced during previous glacial periods, when sea levels were up to 120 m lower than today.
2) Assess the movement of the freshwater-seawater interface under idealised long-term sea-level variations, and compare this to the effects of contemporary changes in onshore heads associated with groundwater extraction.
3) Investigate the potential influence of the Badaminna Fault on the extent and movement of offshore fresh groundwater in the Perth Basin aquifers.

The analysis focuses on changes to the freshwater-seawater mixing zone or 'interface'. Seawater intrusion, the landward movement of the mixing zone, is widely studied for the situation of onshore groundwater conditions, whereas the analysis of seawater intrusion in offshore aquifers is rarely attempted and requires more specialised techniques (Werner et al., 2013; Post et al., 2013). To the authors' knowledge, this is the first time that rates of seawater intrusion in subsea aquifers, associated with paleo conditions and onshore extraction, have been estimated.

2. Study area

Perth is the capital and largest city of Western Australia with a population of about 1.9 million. Water is an increasingly scarce resource across the Perth metropolitan area. Since the mid-1970s, rainfall has declined by 15% leading to a more than 50% reduction in dam inflows (compared to pre-1970s volumes) and a decline in groundwater recharge (de Silva, 2009; Steffen, 2011; CSIRO and Bureau of Meteorology, 2015). This has coincided with rapid growth in Perth's population and in demand for water (ABS, 2015). The decline in rainfall has been linked to anthropogenic climate change and these trends are predicted to continue into the future (Cai and

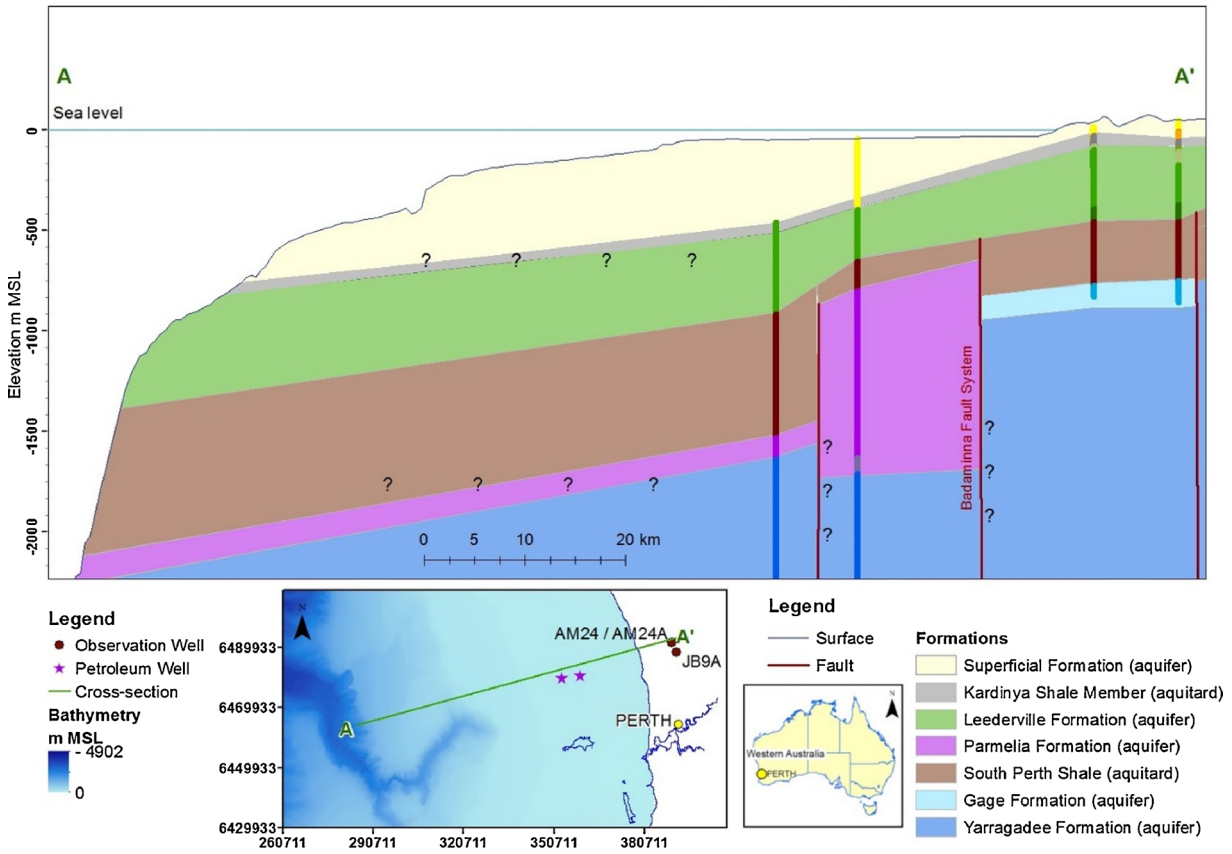

Fig. 1. Offshore stratigraphic cross-section through the Perth Basin. "MSL" refers to mean sea level.

Cowan, 2006; Water Corporation, 2009; Steffen and Hughes, 2013; CSIRO and Bureau of Meteorology, 2015). In recent times, Perth's reticulated water supply is sourced from desalination (47%), groundwater (46%) and dams (7%) (Water Corporation, 2011). Water Corporation (a local water authority) has been increasingly drawing groundwater from the deeper confined aquifers over the past 20 years and estimates that by 2022 groundwater will comprise 50% of Perth's reticulated water supply, most of which will come from confined aquifers (Water Corporation, 2016).

The Perth Basin extends approximately 700 km along the southern part of the West Australian coast. It hosts a Permian to Holocene succession of sedimentary rocks overlying Precambrian basement. Onshore geological and hydrogeological data were used in conjunction with offshore geological information from petroleum exploration wells and seismic data to develop a cross-sectional representation of the offshore stratigraphy in the vicinity of Perth, as shown in Fig. 1. Relative to onshore well logs, the petroleum logs were not particularly high-quality, and at the time this research was undertaken, geophysical logs were not interpreted. This is commonly the case with offshore petroleum logs, because petroleum logging is generally not focussed on interpreting the upper formations. The stratigraphy extends from 10 km onshore to the edge of the continental shelf, approximately 90 km offshore. Fault locations offshore have been inferred from formation offsets. The question marks in Fig. 1 have been added to show that the aquifers/geological units are inferred. Further offshore, where there is no information, layers are inferred and the question marks have been used to highlight this.

Perth has three main aquifers that are used for water supply. These are, in order from deepest to shallowest, the semi-confined Yarragadee aquifer (comprising the Cretaceous Gage Formation, Cretaceous Parmelia Formation and Jurassic Yarragadee Formation), the semi-confined Leederville aquifer (i.e., the Cretaceous Leederville Formation), and the unconfined Superficial aquifer (i.e., Quaternary and Tertiary sediments of the Superficial Formations). The formations comprising the Yarragadee and Leederville aquifers consist of discontinuous, interbedded sandstone, siltstone and shale. The Superficial Formations consist of sand, limestone, silt and clay (Davidson, 1995; Davidson and Yu, 2006). The Cretaceous South Perth Shale (hereafter referred to as the second aquitard) and the Cretaceous Kardinya Shale (hereafter referred to as the first aquitard) are aquitards overlying the Yarragadee and Leederville aquifers, respectively. These aquitards consist of interbedded siltstone and shale. The Yarragadee aquifer is up to 3000 m thick but flow is thought to occur predominantly in the upper 500 m because increasing groundwater salinities beneath this depth suggest a lack of flushing and limited groundwater flow (Davidson, 1995).

Groundwater salinity in the Leederville and Yarragadee aquifers within the onshore portion of the cross section shown in Fig. 1 has changed minimally since the 1980s (Department of Water, 2016b). The measured salinity (in total dissolved solids) in the

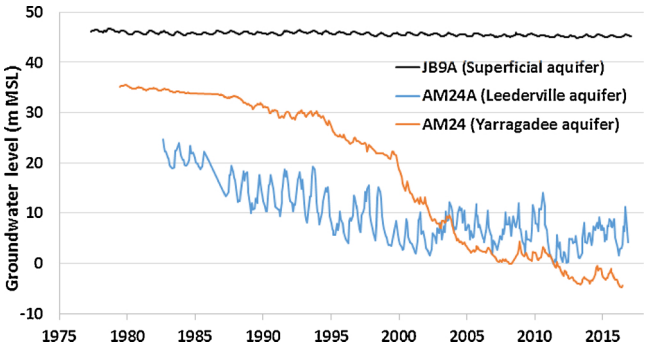

Fig. 2. Groundwater level trends in observation wells located at about 10 km inland from the coast.

Yarragadee aquifer at well AM24 was 200 mg/L in 1983 and 344 mg/L in 2015. The measured salinity in the Leederville aquifer at well AM24A was 200 mg/L in 1983 and 173 mg/L in 2015. Well locations are shown in Fig. 1.

The offshore stratigraphy is modified by the Badaminna Fault system, which is thought to occur about 25 km offshore along the alignment of section AA′ (Fig. 1). Onshore, the Badaminna Fault system is north trending with a steep planar profile and is thought to act as both a barrier to horizontal flow and a conduit for vertical flow from the Yarragadee aquifer into the Leederville aquifer (Leyland, 2012). Bore logs from offshore petroleum exploration wells suggest that the Badaminna Fault occurs in the Yarragadee aquifer and the overlying second aquitard (Fig. 1).

Existing extraction from Perth's confined aquifers has resulted in large head declines since around 1985, when major groundwater extraction commenced. Hydraulic heads prior to 1985 are considered to approximate pre-development conditions for the purposes of this study. In the Yarragadee aquifer, heads have declined by about 40 m since 1985 (as shown in Fig. 2) and are now −5 m MSL (i.e., 5 m below mean sea level) at around 10 km inland from the coast. In the Leederville aquifer, heads at around 10 km inland from the coast have declined by about 20 m since 1985. Despite these declines in head, fresh groundwater continues to be withdrawn in large volumes from wells near the coast in the Yarragadee and Leederville aquifers without evidence of salinization (de Silva, 2009). Given the significant and sustained drawdown proximal to the shoreline caused by pumping, and the lack of salinity impacts, the source of this groundwater is likely to be, at least in part, from beneath the sea. In addition, resistivity logs from offshore petroleum exploration wells offer evidence for groundwater with salinity less than one-third seawater occurring up to 50 km offshore in the Yarragadee aquifer and 20 km offshore in the Leederville aquifer (Hennig and Otto, 2005). This offshore fresh groundwater extent was estimated by Hennig and Otto (2005) as part of a study assessing feasibility of sequestering CO_2 offshore in the Perth Basin aquifers (in the Gage Formation specifically). Formation salinity values were used to infer connectivity of offshore aquifers to onshore recharge areas (lower connectivity is preferential for CO_2 sequestration). A formation salinity value was available for nine petroleum wells in the Leederville aquifer and ten petroleum wells in the Yarragadee aquifer. Hennig and Otto (2005) noted a high degree of uncertainty in these formation salinity values.

Aside from petroleum well bore log data, limited information is available for the offshore portion of the Perth Basin aquifers and aquitards. Hydraulic conductivity, storage and porosity values from a calibrated regional-scale groundwater model of the onshore portion of the aquifer system are shown in Table 1 (Davidson and Yu, 2006; de Silva et al., 2013). These values are presumed, in the absence of offshore aquifer testing, to be broadly representative of the offshore system. Observation wells 10 km inland (Figs. 1 and 2) were used to characterise pre-development and contemporary hydraulic heads in each aquifer.

3. Numerical modelling approach

The variable-density groundwater flow and transport code SEAWAT version 4 (Langevin et al., 2008) was used to explore a number of questions regarding the conceptualisation of the Perth offshore aquifers and accompanying freshwater-seawater relations. SEAWAT is widely used and has been comprehensively tested, and the governing equations are described in the user manual (Guo

Table 1
Parameters used in numerical modelling.

Parameter	Superficial aquifer	First aquitard	Leederville aquifer	Second aquitard	Yarragadee aquifer
Thickness (m)	400	100	500	500	500
Horizontal hydraulic conductivity (m/d)	1	1E-3	1	1E-3	1
Vertical hydraulic conductivity (m/d)	0.1	1E-4	0.1	1E-4	0.1
Specific storage (/m)	5E-5	5E-6	5E-6	1E-6	5E-6
Specific yield (−)	0.25	0.25	0.25	0.25	0.25
Porosity (−)	0.25	0.25	0.25	0.25	0.25
Hydraulic head 10 km inland (pre-development) (m MSL)	46		25		35
Hydraulic head 10 km inland (contemporary) (m MSL)	45		5		−5

and Langevin, 2002). The numerical model domain reflects the aquifer and aquitard thicknesses shown in Fig. 1, although for simplicity, layers are horizontal and the effects of faulting on layer hydraulic properties were initially neglected. The aquifers were assumed to extend 90 km offshore to the continental shelf. A specified-head condition was assigned to both the sea floor and offshore vertical boundary to represent the density and depth-dependent head distribution of the ocean (Langevin et al., 2008). The concentration boundary condition along the sea floor and offshore vertical boundary is one where inflowing water has the concentration of seawater, whereas outflowing water is assigned the ambient concentration of groundwater at the boundary. In this way, seawater inflow to the aquifer causes the coastal boundary cells to approach seawater concentration, whereas groundwater discharge generally causes boundary salinities to fall. Passlow et al. (2005) report that the sea floor in the Perth region is comprised of sandy sediments, and therefore a resistance layer between the aquifer and ocean (as might be formed by a thick layer of mud) was not included within the simulations. The CHD package was used to represent heads at the inland boundary (i.e., 10 km inland from the coast). These were set according to specific scenarios of predevelopment or contemporary onshore conditions, as discussed in the sub-sections that follow.

Numerical modelling adopted longitudinal, horizontal transverse and vertical transverse dispersivities of 50 m, 5 m and 0.5 m, respectively, consistent with estimates for systems of this scale (Gelhar et al., 1992). The molecular diffusion coefficient was set to 8.64×10^{-5} m^2/d, which is the same as that used by Michael et al. (2016) for modelling subsea aquifers. The temperature of the water was assumed to be 25 °C.

The cross-sectional model domain was uniformly discretised using 500 vertical columns of 200 m width, and 40 horizontal layers of 50 m thickness. Voss and Souza (1987) suggest that a mesh Peclet number that is calculated in the direction of flow, i.e., using the longitudinal dispersivity, should be 4 or less, and we are within that criteria. Voss and Souza (1987) also suggest that the Peclet number calculated using the transverse dispersivities should be 10 or less. We have achieved this for the horizontal transverse dispersivity, which is 10. However, we do not abide by this criteria for the vertical transverse dispersity, for which the Peclet number is 100. It is worth noting here that Voss and Souza (1987) also say that 'this stringent criteria has been violated in most published transport simulations'. Simulation times for the transient models were very long and therefore a compromise between model run times and discretisation was made, which has resulted in a larger than ideal Peclet number in the vertical transverse direction. Effects of grid discretization were tested through the application of alternative grid resolutions, indicating that the results are not grid dependent. The Strongly Implicit Procedure and General Conjugate Gradient solvers were selected for flow and transport calculations, respectively (Guo and Langevin, 2002). The Total-Variation Diminishing advection package was used with a Courant number of 0.75, where a Courant number less than or equal to one is generally required to limit numerical dispersion and achieve accurate results (Zheng and Bennett, 2002).

3.1. Preliminary steady-state simulations

Over the past half million years, sea level in the Perth region has varied between around 0 m MSL (i.e., current levels) and −120 m MSL (i.e., during glacial periods) (Smith et al., 2011). Lower sea levels are generally thought to cause an increase in water table gradients and enhanced topographically driven flow (Post et al., 2013). Therefore, groundwater flow in the offshore direction may have increased in the Perth aquifers during periods of lower sea levels. This would require greater rates of recharge, partly a consequence of the exposure of the continental shelf to rainfall infiltration, amongst other complicating factors (Post et al., 2013). In addition, the coastline would likely have been further offshore leading to a more distant source of seawater. Initially, the potential for emplacement of fresh groundwater within the Perth offshore aquifers arising under the current sea level and during lower sea-level stands was explored by modelling the steady-state salinity distribution for sea levels of 0 m MSL, −60 m MSL and −120 m MSL. These three sea levels represent approximate end-members of long-term sea-level variation (i.e., 0 m MSL and −120 m MSL) and an average of long-term sea-level variation (i.e., −60 m MSL). The average value of −60 m MSL was obtained from the sea-level fluctuations derived by Smith et al. (2011) for the period 450 ky bp to the present day. It is worth noting here that glaciation did not occur in the Perth region during the Pleistocene (Colhoun and Barrows, 2011), which is the period that spans the world's most recent period of repeated glaciations.

The position of the coastline was approximated as being 20 km and 40 km further offshore than the current shoreline for sea levels of −60 m MSL and −120 m MSL, respectively, based on present day bathymetry (Fig. 1). Steady-state conditions were obtained by long-term transient simulations, using stable heads, that were continued until movements of the interface tip (i.e., the intersection between the 50% seawater isochlor and the top of the aquifer) and interface toe (i.e., the intersection between the 50% seawater isochlor and the base of the aquifer) were less than 10 m in 10 ky within the Leederville and Yarragadee aquifers. This required simulation periods of 1200 ky, 460 ky and 260 ky for the 0 m MSL, −60 m MSL and −120 m MSL sea levels, respectively. Predevelopment heads detailed in Table 1 were used at the inland boundary for simulations that adopted the sea levels given above. The initial concentration was set equal to seawater throughout the model domain and the initial heads was set equal to the adopted sea level of each simulation.

3.2. Transient simulations of sea-level change

A transient sea-level change scenario was used to explore the movement of the interface associated with sea-level variation since the last glacial maximum. The last glacial maximum occurred approximately 20 ky bp, with a sea level around 120 m lower than today (Yokoyama et al., 2000; Smith et al., 2011). A linear change in sea level from –120 m MSL to 0 m MSL was simulated over the period from 20 ky bp to the year 1985. The year 1985 is selected as it approximates the end of the predevelopment period, in terms of

onshore heads, as detailed above. The model was then run for a further 100 ky with constant boundary conditions (i.e., a sea level of 0 m MSL and predevelopment inland heads) in order to explore the time required to reach steady state following the sea-level change. The first 20 ky of the simulation period was divided into 10 stress periods of equal length. The subsequent 100 ky of the simulation period was also divided into 10 stress periods of equal length. Each stress period had 10,000 time steps. The time-variant specified-head package (CHD) of SEAWAT was used to implement the linear change in sea level within the first 20 ky of the simulation period. To simulate the changing position of the shoreline (induced by the change in sea level), the concentration boundary and time-variant specified-head boundary were extended landward by 4 km during each of the first 10 stress periods (representing a 40 km linear shift in coastline over the initial 20 ky period). The present day bathymetry was used to derive the offshore position of the coastline under past sea level low stands. Mitchell et al. (2007) have reported that the sediment accumulation rate on the Gippsland shelf (in south east Australia) was about 2–4 cm/ky, and accumulation rates on the Perth shelf are likely to be similar. Therefore, over the period of the transient simulation, which starts 20 ky bp, the geomorphology and bathymetry are not likely to have changed significantly relative to the modern day. Predevelopment heads were used at the inland boundary over the entire simulation period. The steady-state head and concentration distributions for a sea level of −60 m MSL were used as initial conditions because, as described above, this approximates average sea level for the past 450 ky in the Australian region. To summarise, this simulation involved using initial conditions of the steady-state result for −60 m MSL and a linear increase of the sea level from −120 m MSL to 0 m MSL (accompanied by a linear change in coastline position) over a simulation period from 20 ky bp to the year 1985, with an additional simulation time of 100 ky with constant boundary conditions.

3.3. Transient simulations of onshore head changes

A transient onshore head change scenario was used to explore the relationship between inland head decline (due to groundwater extraction) and seawater intrusion within Perth's offshore aquifers. The simulation period was from 20 ky bp to 100 ky after present. The model was set up identical to the transient sea-level change scenario model, described above, for the period 20 ky bp to 1985. From 1985 to 2015, inland heads were reduced linearly from predevelopment to contemporary values (see Table 1), and then held constant at contemporary values to the end of the simulation period. A 30-year head decline period was used to approximately match the measured period of head decline from 1985 to contemporary times (shown in Fig. 2). The simulation involved 21 stress periods. The first 10 stress periods are the same as the transient sea-level scenario model. The 11^{th} stress period (of length 30 y) had the inland head decline from predevelopment to contemporary levels and a sea level of 0 m MSL. The remaining stress periods, of approximately equal length, had inland heads constant at contemporary levels and a sea level of 0 m MSL. Each stress period had 10,000 time steps.

3.4. Impact of the badaminna fault

A number of additional steady-state simulations with a sea level of −60 m MSL were carried out to explore the potential influence of the Badaminna Fault on offshore salinity distributions. The Badaminna Fault was implemented as a 1 km wide vertical column located 25 km offshore within both the Yarragadee aquifer and second aquitard. The fault was conceptualized as a barrier to horizontal flow and conduit to vertical flow, consistent with the findings of Leyland (2012). Horizontal hydraulic conductivity was decreased by a factor of 1000 to simulate the fault as a barrier to horizontal flow, while vertical hydraulic conductivity was increased by a factor of 1000 to simulate the fault as a conduit to vertical flow. This conceptualization conforms to the best available, although limited, information regarding the Badaminna Fault, as described in Section 2.

Transient simulations with sea-level change (see Section 3.2) and onshore head changes (see Section 3.3) were repeated with the Badaminna Fault included.

4. Results

4.1. Steady-state simulations

These simulations predict the steady-state interface positions under predevelopment inland heads and sea levels of −120 m MSL, −60 m MSL and 0 m MSL, for the idealised conceptual model used in this study. The modelled steady-state salinity distribution and velocity vectors for sea levels of −120 m MSL, −60 m MSL and 0 m MSL are shown in Fig. 3a–c, respectively. In each sea-level case, the Superficial aquifer is salinized in the offshore component, as expected due to the lack of an overlying aquitard. Freshwater from the Leederville aquifer seeps upwards into the overlying Superficial aquifer, causing complex upwelling and mixing processes due to buoyancy effects. This is shown as oscillations in the 80% seawater isochlor within the Superficial aquifer, and by the directions of the velocity vectors. The shoreline is further landward in cases with higher sea levels, commensurate with the seabed slope.

Velocity vectors from the steady-state simulations shown in Fig. 3 demonstrate that, as expected, the magnitude of flow velocity in the offshore direction decreases with increasing sea level, in both the Leederville and Yarragadee aquifers. The direction of groundwater movement in the Leederville and Yarragadee aquifers switches within the interface, whereby groundwater flows landward on the seaward side of the interface, and flows offshore on the landward side of the interface. Also, in general, groundwater seeps upward through aquitards landward of the interface, and seeps downward seaward of the interface.

Table 2 gives results for the interface tip and toe positions relative to the furthest offshore aquifer extent (i.e., the edge of the continental shelf) in the Leederville and Yarragadee aquifers and under the different sea levels. At sea levels of −120 m MSL and −60 m MSL, the steady-state tip and toe in both aquifers are predicted to be within 3 km and 25 km, respectively, of the furthest

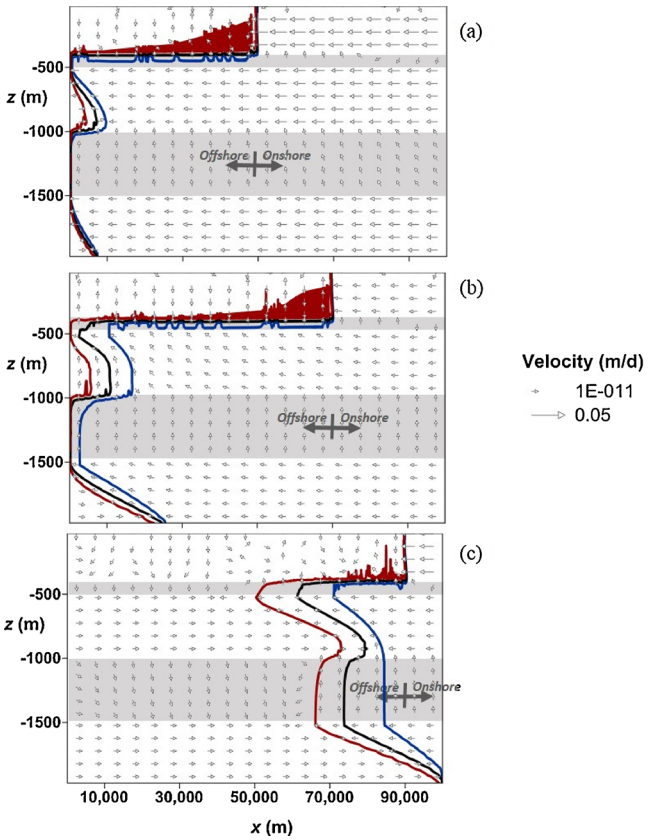

Fig. 3. Distribution of the 20% (blue line), 50% (black line) and 80% (red line) relative salinity contours for the steady-state salinity distributions corresponding to sea levels of: (a) −120 m MSL, (b) −60 m MSL, and (c) 0 m MSL. Velocity vectors are shown for every 25th column and 2nd layer using a log scale. Grey shading identifies aquitards.

Table 2
Predicted steady-state interface tip and toe locations (distances are taken from the edge of the continental shelf; 90 km offshore from the present coastline) in the Leederville and Yarragadee aquifers under different sea levels.

Sea level (m MSL)	Shoreline location (from present day) (km)	Leederville aquifer		Yarragadee aquifer	
		Tip (m)	Toe (m)	Tip (m)	Toe (m)
−120	40	300	6400	300	7300
−60	20	2600	10,600	400	24,700
0	0	61,400	79,200	73,900	99,900

offshore aquifer extent (i.e., 90 km offshore from the present coastline). That is, under sea levels of −120 m MSL and −60 m MSL, freshwater is predicted to extend to more than 87 km and 65 km, respectively, from the present day coastline position. Given these results, and the lengthy periods during which low sea levels persisted during the Pleistocene, the Perth confined aquifers were most likely extensively freshened under glacial sea-level low stands.

The interface position obtained for a sea level of 0 m MSL is considerably more landward than the interface positions for sea levels of −120 m MSL and −60 m MSL. For example, the toe in the Yarragadee aquifer was estimated to be about 17 km further landward under a sea level of −60 m MSL compared to a sea level of −120 m MSL, and about 75 km further landward under a sea level of 0 m MSL compared to a sea level of −60 m MSL. In the steady-state simulations, freshening of the Perth confined offshore aquifers during glacial sea-level low stands arises from both the shift in the coastline and the increased hydraulic gradient between the onshore and offshore boundary heads.

Any assessment of hydraulic gradients between offshore and onshore boundaries requires consideration of water density effects on groundwater heads. As detailed by Post et al. (2007), the equivalent freshwater head can be calculated as:

$$h_f = z + (h - z)\frac{\rho_s}{\rho_f} \quad (1)$$

Table 3
Equivalent freshwater heads (h_f) along the vertical offshore boundary under different sea levels.

Sea level (m MSL)	Leederville		Yarragadee	
	Top (m MSL)	Base (m MSL)	Top (m MSL)	Base (m MSL)
−120	−110.5	−98	−85.5	−73
−60	−49	−36.5	−24	−11.5
0	12.5	25	37.5	50

Here z [L] is the depth (below datum, equal to the current sea level in this study) at which the equivalent freshwater head is obtained, h [L] is the elevation of the sea level (above the datum), and ρ_s [M/L^3] and ρ_f [M/L^3] are seawater and freshwater densities, respectively. In horizontal aquifers, h_f can be compared to onshore (freshwater) water levels to discern whether the steady-state freshwater flow is onshore or offshore. For example, at the base of the Leederville aquifer at the offshore boundary, $h_f = -98$ m if the sea level (h) is -120 m, $z = -1000$ m, $\rho_s = 1025$ kg/m^3 and $\rho_f = 1000$ kg/m^3. Table 3 lists h_f values for the top and base of the Leederville and Yarragadee aquifers at the offshore vertical boundary under different sea levels. The reduction in h_f is 61.5 m at each location for a 60 m change in sea level, as expected from Eq. (1). For a sea level of 0 m MSL, h_f at the Yarragadee aquifer base at the offshore boundary (= 50 m MSL) is larger than the inland boundary head (h = 35 m MSL). Under these conditions, it is expected that seawater will reach the inland boundary (Werner, 2017). Further, it is expected that the entire thickness of the offshore aquifer will be salinized if onshore heads are less than h_f at the Yarragadee aquifer top at the offshore boundary (= 37.5 m MSL). However, as shown in Fig. 3c, groundwater of salinity less than 50% seawater is predicted to occur near the inland boundary at this sea level. As such, the Yarragadee aquifer is almost, but not completely, salinized. The sharp-interface analytic solutions used by Werner (2017) are known to over-predict the inland interface position and they also do not account for inter-aquifer interactions. These are likely the reasons for the discrepancy between the predicted inland interface extent from the theory of Werner (2017) and that modelled numerically here.

The interface width (i.e., the distance between the 20% and 80% seawater isochlors) produced by SEAWAT is larger with increasing sea level, as shown in Table 4. For example, in the Leederville aquifer the width of the wedge toe increases from 5.4 km at a sea level of −120 m MSL to 11.2 km at a sea level of −60 m MSL, to 12.6 km at a sea level of 0 m MSL. This increased interface width is associated with the reduced gradient as the sea level increases. Under sea levels of −120 m MSL and −60 m MSL, the interface tip in the Leederville and Yarragadee aquifers reaches the offshore continental boundary and therefore the width of the interface tip will be influenced by the boundary to some degree. However, this has been minimised by the choice of concentration boundary condition, described in Section 3.

4.2. Transient simulation of sea-level change

This simulation predicts the movement of the interface under predevelopment inland heads (as assumed to have occurred up to 1985), with rising sea levels over the past 20,000 years (i.e., since the last glacial maximum). Fig. 4 shows the predicted salinity distribution in 1985 and at 10 ky after present (i.e., 10 ky after 2015). It is recognised that predictions 10 ky into the future are not especially useful from a management perspective, but they nonetheless provide an indication of the predicted propensity for the interface to migrate over long periods due to past sea-level changes and, as detailed in the next section, relative to interface changes caused by groundwater extraction.

Fig. 4a shows that the model predicts a large body of offshore fresh groundwater, extending almost to the edge of the continental shelf, under predevelopment conditions (i.e., in 1985). The interface tip is predicted to occur within 5 km of the aquifers' offshore limit in both the Leederville and Yarragadee aquifers, while the interface toe is predicted to occur within 18 km and 28 km of the offshore limit in the Leederville and Yarragadee aquifers, respectively. This simulation produces an offshore fresh groundwater extent that is significantly larger than measured values reported by Hennig and Otto (2005), detailed above in Section 2.

Rates of interface movement are given in Table 5. To enable comparison over time, the rates of interface movement are detailed separately for the predevelopment (20 ky bp to 1985), current (1985–2015) and future (2015 to 10 ky after present) periods. To be clear, these rates of interface movement (for all periods) relate to the influence of paleo sea-level change only. The onshore heads were held at 1985 levels for the entire simulation and only sea level was changed. The additional impact of pumping on interface movement in the current and future periods is assessed in the next section through comparison with results presented here.

Table 4
Interface width at the tip and toe under different sea levels.

Sea level (m MSL)	Leederville		Yarragadee	
	Tip (km)	Toe (km)	Tip (km)	Toe (km)
−120	0.6	5.4	0	0.7
−60	10.3	11.2	2.6	3.1
0	21.0	12.6	18.4	0.8

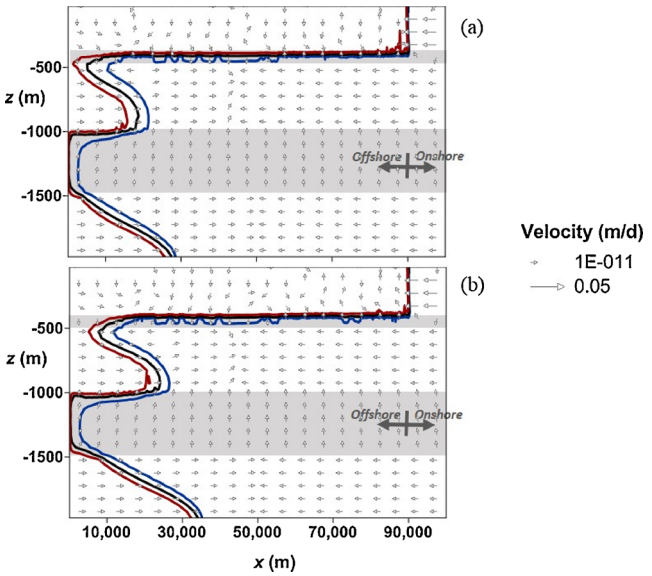

Fig. 4. Distribution of the 20% (blue line), 50% (black line) and 80% (red line) relative salinity contours for the transient simulation at times: (a) 1985 and (b) 10 ky after present. Velocity vectors are shown for every 25th column and 2nd layer using a log scale. Grey shading identifies aquitards.

Table 5
Predicted rate of interface movement associated with paleo sea-level change for different time periods during the simulation.

Time period	Sea level (m MSL)	Leederville tip (m/y)	Leederville toe (m/y)	Yarragadee tip (m/y)	Yarragadee toe (m/y)
20 ky bp to 1985	−120 to 0	0.14	0.37	0.23	0.14
1985 to 2015	0	0.2	0.63	0.42	0.74
2015 to 10 ky after present	0	0.24	0.57	0.48	0.67

The model predicts that the interface in both the Leederville and Yarragadee aquifers is still moving landward in response to rising sea levels since the last glacial maximum (20 ky bp). The maximum predicted rate of interface movement (i.e., for the tip and toe in the Leederville and Yarragadee aquifers) for the predevelopment, current and future periods is 0.37 m/y, 0.74 m/y and 0.67 m/y, respectively. The modelled interface had not reached the corresponding steady-state interface position (i.e., for a sea level of 0 m MSL and predevelopment inland heads; Fig. 3c) after 100 ky (salinity distribution not shown for brevity).

4.3. Transient simulations of onshore head changes

This simulation predicts the movement of the interface under the influence of paleo sea-level change and extraction (i.e., heads declining due to 30 years of onshore extraction). Fig. 5a shows a comparison of the 2015 salinity distributions under extraction and no-extraction scenarios. Differences in the predicted tip and toe positions at 2015 are barely detectable (see Fig. 5a).

Fig. 5b shows the predicted salinity distributions under the extraction and no-extraction scenarios at 10 ky after present. Extraction is predicted to cause the interface to move further landward in both aquifers, as expected. The interface tip moved further landward by around 1 km and 3.5 km in the Leederville aquifer and Yarragadee aquifers, respectively. Extraction causes the interface toe to move landward by similar distances (1 km and 3.1 km, respectively).

Table 6 details rates of interface movement for the current (1985–2015) and future (2015 to 10 ky after present) periods. Through comparison with the values in Table 5, it can be seen that the onshore head change is not predicted to have significantly increased the rate of interface movement during the current period. However, for the future period, the onshore head change is predicted to increase interface movement by 37% at the Leederville tip, 16% at the Leederville toe, 75% at the Yarragadee tip and 48% at the Yarragadee toe. As such, extraction-induced changes in onshore heads are expected to eventually cause a significant increase in seawater intrusion within offshore aquifers of the Perth Basin, for the conceptualisation and aquifer parameters used here.

The predicted rates of offshore seawater intrusion that were obtained from the modelling are slower than reported rates of seawater intrusion in onshore aquifers, although only a few cases are available for comparison. For example, a well-documented case of seawater intrusion associated with pumping in Cape May County (USA; Barlow and Reichard, 2010) found that the 250 mg/L chloride isochlor moved inland at a rate of about 40 m/y during 1940–1990. In another well-documented case of pumping-induced seawater intrusion in the upper aquifer of Ventura County (USA), the 250 mg/L chloride isochlor moved inland by up to 150 m/y (Izbicki, 1996).

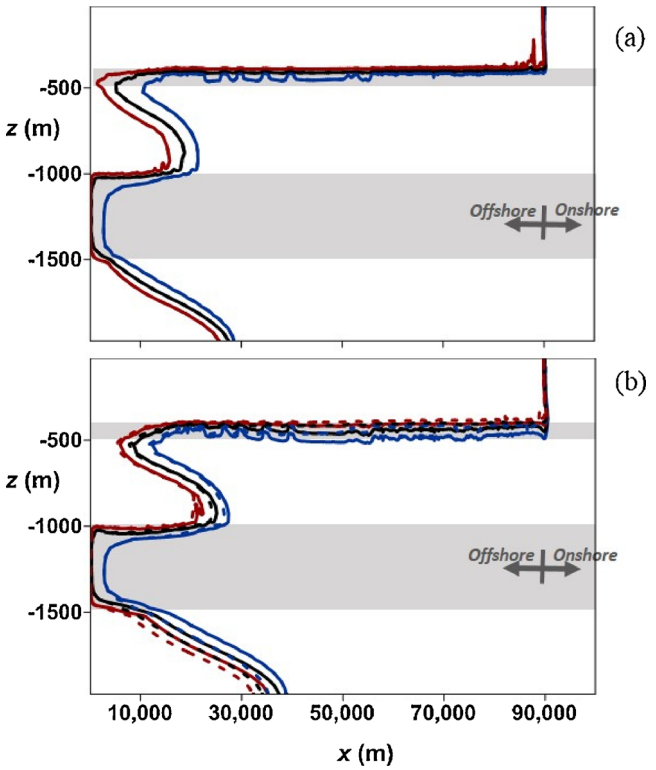

Fig. 5. Distribution of the 20% (blue line), 50% (black line) and 80% (red line) relative salinity contours for the transient simulation with extraction (solid line) and no-extraction (dashed line) at times: (a) 2015, and (b) 10 ky after present. Grey shading identifies aquitards.

Table 6
Predicted rates of interface movement associated with paleo sea-level change and onshore head changes for different time periods during the simulation.

Time period	Leederville tip (m/y)	Leederville toe (m/y)	Yarragadee tip (m/y)	Yarragadee toe (m/y)
1985 to 2015	0.2	0.63	0.42	0.74
2015 to 10 ky after present	0.33	0.66	0.84	0.99

4.4. Impact of the Badaminna Fault

Results of the steady-state simulations that included the Badaminna Fault are shown in Fig. 6. As expected, the fault significantly reduced the predicted offshore extent of fresh groundwater in the Leederville and Yarragadee aquifers when compared to the results from the equivalent steady-state simulation without the fault (Fig. 3b). With the fault, the interface tip is predicted to be 14 km and 63 km further landward in the Leederville and Yarragadee aquifers, respectively, relative to the corresponding simulation without the

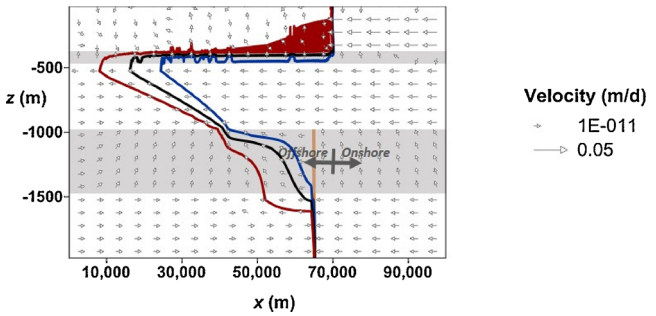

Fig. 6. Distribution of the 20% (blue line), 50% (black line) and 80% (red line) relative salinity contours for the steady-state simulation with a sea level of −60 m MSL, with the Badaminna Fault located at x = 65,000 m (shown as an orange line). Velocity vectors are shown for every 25th column and 2nd layer using a log scale. Grey shading identifies aquitards.

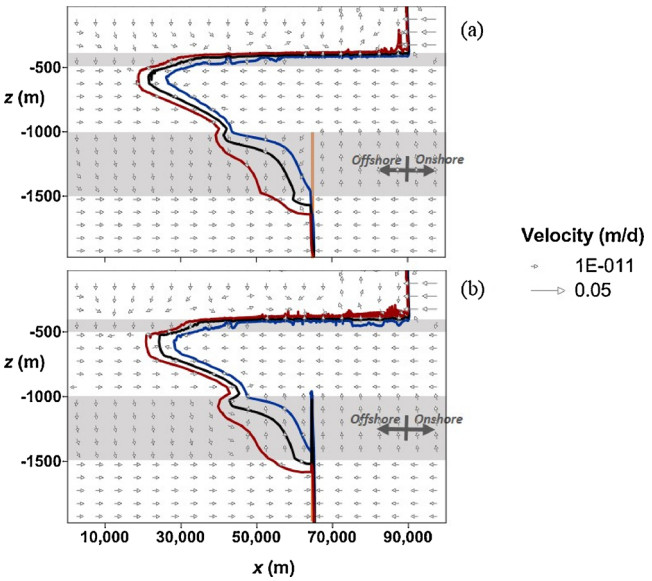

Fig. 7. Distribution of the 20% (blue line), 50% (black line) and 80% (red line) relative salinity contours for the transient simulation with the Badaminna Fault at times: (a) 1985 and (b) 10 ky after present. Velocity vectors are shown for every 25th column and 2nd layer using a log scale. Grey shading identifies aquitards. The Badaminna Fault is located at x = 65,000 m (shown as an orange line).

fault. The interface toe is predicted to be 30 km and 41 km further landward in the Leederville and Yarragadee aquifers, respectively. In the Yarragadee aquifer, the flow towards the offshore is being obstructed by the fault, as expected, especially at the base of the aquifer. Velocity vectors indicate that flow direction within the fault is vertical upward.

The fault increased the predicted mixing zone width at the tip of the Leederville and Yarragadee aquifers, when compared to the steady-state simulation results without the fault. Conversely, the fault reduced the predicted mixing zone width at the toe in both the Leederville and Yarragadee aquifers. These results add to the results of recent sand tank experiments by Houben et al. (2018) who found wider mixing zones along an impermeable fault.

A transient simulation was carried out to explore the influence of the Badaminna Fault on offshore fresh groundwater under sea-level variation since the last glacial maximum (20 ky bp). Fig. 7a and b show that at 1985 and 10 ky after present, respectively, the interface in the Leederville and Yarragadee aquifers is significantly further landward than the interface position predicted by the corresponding transient simulation without the Badaminna Fault, as expected (Fig. 4a and b). The predicted salinity distribution for 1985 is more in line with the measured extent of offshore fresh groundwater presented by Hennig and Otto (2005) than results obtained from the transient simulation without the fault (Section 4.2). These results also highlight the previously unexplored potential for offshore faults to have a significant impact on offshore fresh groundwater extent.

At 10 ky after present, groundwater of higher salinity (i.e., greater than 20% seawater salinity) is simulated within the Badaminna fault and this spike in salinity is caused by the high vertical conductivity within the fault. The salinity spike follows the dimensions of the Badaminna fault, which is 1 km wide and occurring within the Yarragadee aquifer and overlying second aquitard. This spike in salinity has also penetrated into the base of the Leederville aquifer, above the simulated Badaminna Fault. This indicates that the fault is predicted to act as a conduit for higher salinity groundwater to enter the Leederville aquifer from the underlying aquitard and aquifer. This form of salinization has been previously documented in the onshore section of the Floridan aquifer system in south eastern Georgia and north eastern Florida, USA (Barlow and Reichard, 2010). At that location, fractures and faults have been shown to provide a pathway for high salinity water to migrate from a lower confined aquifer upward into shallower confined aquifers, especially when pumping has lowered the heads in these overlying aquifers.

Rates of interface movement for the transient simulation with the Badaminna Fault are shown in Table 7. The simulation predicts that the interface in the Leederville and Yarragadee aquifers is still moving landward in response to rising sea levels since the last

Table 7
Predicted rate of interface movement associated with paleo sea-level change for different time periods during the simulation, for the simulation with the Badaminna Fault.

Time period	Leederville tip (m/y)	Leederville toe (m/y)	Yarragadee tip (m/y)	Yarragadee toe (m/y)
20 ky bp to 1985	0.26	0.06	0.004	0.001
1985 to 2015	0.13	0.31	0.05	0.001
2015 to 10 ky after present	0.29	0.32	0.47	0.02

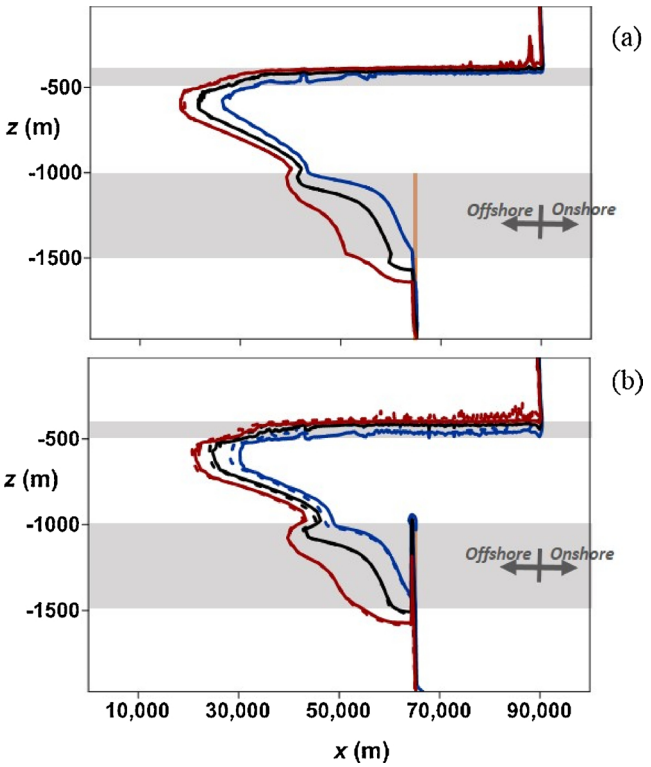

Fig. 8. Distribution of the 20% (blue line), 50% (black line) and 80% (red line) relative salinity contours for the transient simulation with the Badaminna Fault under extraction (solid line) and no-extraction (dashed line) at times: (a) 2015 and (b) 10 ky after present. Grey shading identifies aquitards. The Badaminna Fault is located at x = 65,000 m (shown as an orange line).

glacial maximum (20 ky bp), although at a negligible rate for the Yarragadee toe. Rates of interface movement with the fault are slower than those predicted by the simulation without the fault (Table 5), with the exception of the Leederville tip over the periods 20 ky bp to 1985 and 2015 to 10 ky after present.

A transient simulation was carried out to explore the influence of the Badaminna Fault on offshore fresh groundwater under sea-level variation since the last glacial maximum and declines in onshore heads associated with groundwater extraction. Fig. 8a shows a comparison of the salinity distribution at time 2015 under the extraction and no-extraction scenarios, with the Badaminna Fault. There is no measurable difference between interface positions.

Fig. 8b shows the predicted salinity distribution under the extraction and no-extraction scenarios, with the Badaminna Fault, at 10 ky after present. Extraction is predicted to cause the interface tip to move further landward by around 1 km in the Leederville and 0 km in the Yarragadee aquifer. Extraction causes the interface toe to move landward by 1 km in the Leederville aquifer and 0 km in the Yarragadee aquifer. These values are significantly smaller than those obtained from the simulation without the fault (Section 4.3). After 10 ky, extraction is predicted to increase, albeit marginally, the size of the plume of higher salinity groundwater moving upward through the fault into the Leederville aquifer.

Table 8 details rates of interface movement for the current (1985–2015) and future (2015 to 10 ky after present) periods for the extraction scenario with the Badaminna Fault. These rates are lower than those for the corresponding simulation without the Badaminna Fault (Table 6), with the exception of the Leederville tip for the period 2015 to 10 ky after present. Extraction-induced reductions in inland head are causing seawater intrusion at a rate that is up to 50% faster than under paleo-conditions alone, with the Badaminna Fault implemented in the model.

Table 8
Predicted rate of interface movement associated with paleo sea-level change and onshore head changes for different time periods during the simulation, for the simulation with the Badaminna Fault.

Time period	Leederville tip (m/y)	Leederville toe (m/y)	Yarragadee tip (m/y)	Yarragadee toe (m/y)
1985 to 2015	0.13	0.31	0.05	0.001
2015 to 10 ky after present	0.33	0.41	0.53	0.03

Table 9
Steady-state flux through the inland boundary for each aquifer under different sea-level conditions.

Aquifer	Inland boundary flux (m^2/d) for 0 m MSL sea level	Inland boundary flux (m^2/d) for −60 m MSL sea level	Inland boundary flux (m^2/d) for −120 m MSL sea level
Superficial	1.7	1.23	1.03
Leederville	0.12	0.66	0.84
Yarragadee	0.05	0.50	0.81

5. Discussion

5.1. Inland boundary condition

There is limited information relating to groundwater recharge and aquifer fluxes for the Perth aquifers. For this reason, groundwater heads, for which there is information since around the mid-1980s, have been used instead of fluxes in assigning the inland boundary condition for all models detailed in the above sections. The use of a specified-head inland boundary means that fluxes through the aquifer system vary under different sea levels. For the steady state simulations of different sea levels, the flux through the inland boundary increased significantly within the Leederville and Yarragadee aquifers as the sea level declined, as shown in Table 9. For example, in the Yarragadee aquifer, the flux increased from 0.05 m^2/d for a sea level of 0 m MSL, to 0.50 m^2/d for a sea level of −60 m MSL, and to 0.81 m^2/d for a sea level of −120 m MSL. In contrast to the Leederville and Yarragadee aquifers, there is a decrease in flux within the Superficial aquifer with declining sea level. This is due to a reduction in the saturated aquifer thickness within the unconfined Superficial aquifer, associated with the lower sea levels.

It is not possible to compare the simulated rates of flux, shown in Table 9, with onshore groundwater recharge rates, because recharge rates into the Leederville and Yarragadee aquifers are unknown, including under both current and paleo-conditions. These aquifers most likely receive recharge via areas where they outcrop or sub-crop inland of the coastal zone as well as in areas where the overlying or underlying aquitards are thin, absent or intersected by conductive faults. To estimate the cumulative recharge to these aquifers inland of our landward boundary, recharge rates would need to be multiplied by respective areas of outcrop and sub-crop, which are not well known for the Leederville and Yarragadee aquifers, and the corresponding rates of recharge have never been estimated. Unfortunately, these complex and poorly characterised recharge mechanisms make it virtually impossible to compare simulated flux rates with recharge rates into the Leederville and Yarragadee aquifers.

To explore the influence of the choice of inland boundary condition on interface position and movement, additional simulations were carried out where the inland boundary was set up as a specified-flux boundary. The specified flux used in the modelling was based on the flux from the specified-head simulation that adopts a sea level of 0 m MSL and a pre-development inland head. That is, we presumed that the rate of discharge to the sea during sea-level low-stands was equivalent to the predevelopment freshwater discharge to the sea, under modern sea-level conditions. By adding specified-flux simulations to the list of modelling scenarios, we aim to capture the “end-member” situations, namely: (a) steeper hydraulic gradients under lower sea levels (i.e., as per Post et al., 2013), and (b) the same hydraulic gradient at the inland boundary regardless of the sea level. We expect that the reality of the changes to head and flux within the aquifer system under changing sea level will be somewhere in between these two conditions.

As expected, under specified-flux inland boundary conditions, the simulated interface was further landward for sea levels of −60 m MSL and −120 m MSL, when compared to the specified-head simulations. This is evident from a comparison of Figs. 3 and 9, and Tables 3 and 10. This arises because the seaward groundwater flow was lower in the specified-flux simulations compared to the corresponding (i.e., same sea level) specified-head simulation. For example, for a sea level of −120 m MSL the seaward groundwater flow in the Yarragadee aquifer was 0.05 m^2/d in the specified-flux simulation, whereas the corresponding specified-head simulation, involving steepening of the gradient, had a seaward groundwater flow of 0.81 m^2/d. Thus, the lower seaward discharge of the specified-flux situation led to a landward shift in the interface.

Additionally, a transient simulation was run using the specified-flux inland boundary condition to assess rates of inland interface movement for the predevelopment (20 ky bp to 1985), current (1985–2015) and future (2015 to 10 ky after present) periods. The results are shown in Table 11. The reduced seaward flux of specified-flux boundary conditions produced slower interface movements under paleo sea-level changes. That is, under specified-flux conditions, the maximum predicted rate of interface movement for the predevelopment, current and future periods is 0.13 m/y, 0.32 m/y and 0.29 m/y, respectively. These rates are 35%, 43% and 43% of the maximum predicted rates of interface movement for the predevelopment, current and future periods under specified-head conditions (as detailed in Section 4.2). This result is caused by the reduction in seaward flux of freshwater as the sea rises in specified-head simulations, thereby enhancing seawater intrusion relative to specified-flux simulations, in which the seaward flux is constant despite rising sea levels.

Simulations that consider interface movement associated with onshore head changes since 1985 under specified-flux inland boundary conditions were not carried out. By their nature, these simulations require a change of head at the inland boundary rather than altered flux at the inland boundary. While we prefer not to include this simulation, a possible approach may be to use the

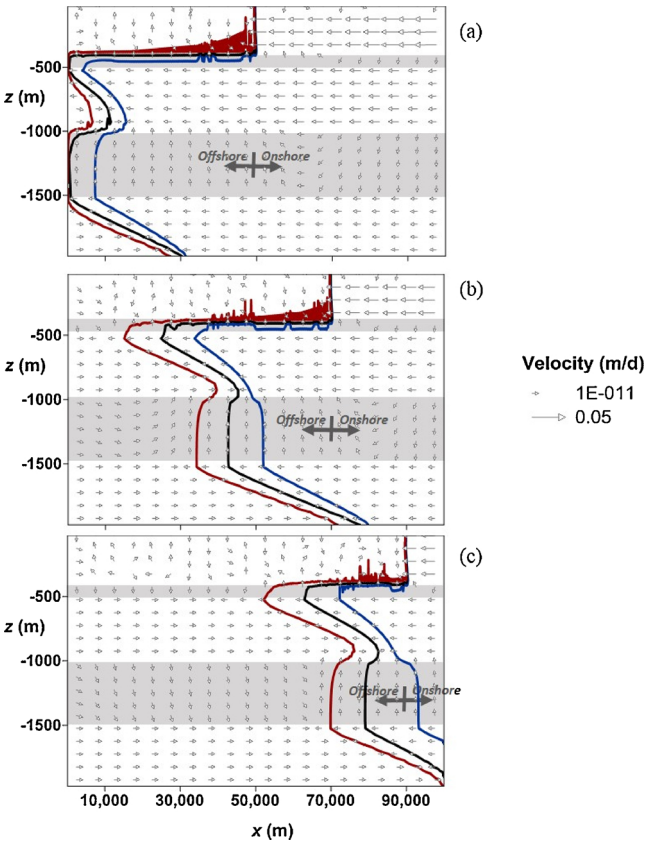

Fig. 9. Distribution of the 20% (blue line), 50% (black line) and 80% (red line) relative salinity contours for the steady-state salinity distributions corresponding to sea levels of: (a) −120 m MSL, (b) −60 m MSL, and (c) 0 m MSL. Velocity vectors are shown for every 25th column and 2nd layer using a log scale. Grey shading identifies aquitards. A specified flux was used at the inland boundary for these simulations.

Table 10
Predicted steady-state interface tip and toe locations (distances are taken from the edge of the continental shelf; 90 km offshore from the present coastline) in the Leederville and Yarragadee aquifers under different sea levels, and a specified-flux inland boundary condition.

Sea level (m MSL)	Shoreline location (from present day) (km)	Leederville aquifer		Yarragadee aquifer	
		Tip (m)	Toe (m)	Tip (m)	Toe (m)
−120	40	600	11,000	1000	30,300
−60	20	25,200	45,400	42,800	76,600
0	0	63,000	82,360	79,200	100,000

Table 11
Predicted rates of interface movement associated with paleo sea-level change for different time periods during the simulation, with a specified-flux inland boundary.

Time period	Sea level (m MSL)	Leederville tip (m/y)	Leederville toe (m/y)	Yarragadee tip (m/y)	Yarragadee toe (m/y)
20 ky bp to 1985	−120 to 0	0.13	0.1	0.08	0.01
1985 to 2015	0	0.16	0.31	0.32	0.22
2015 to 10 ky after present	0	0.22	0.29	0.19	0.21

specified-head simulations to determine the change of flux that occurs at the inland boundary due to the change of head associated with onshore pumping and then apply this flux change within the specified-flux simulations. However, we expect these two approaches to produce essentially the same effect on the interface because, in both cases, the flux and the head at the inland boundary will change by the same amount.

5.2. Limitations

The results presented here are the outcome of simulations that represent a necessarily limited conceptualisation and parameterisation of the Perth offshore aquifer system. A range of factors have not been considered including small-scale heterogeneities (i.e., within the layers) associated with, for example, deposition and erosion processes. The aquifers have been modelled as having homogeneous hydraulic parameters despite that the hydraulic conductivity and porosity may decrease with depth in each aquifer, for example. The influence of the offshore paleo-channel (shown in Fig. 1) has not been explicitly considered, even though this geomorphic feature may act as a preferential path for salinization of the Superficial aquifer offshore. The Badaminna Fault has been explicitly included in the simulations using a single realisation of hydraulic properties. An uncertainty analysis exploring the relationship between fault hydraulic properties, amongst a number of other uncertainties, and offshore fresh groundwater extent is considered beyond the scope of this study.

It is not possible to know the initial conditions 20 ky bp and hence an assumption was made for the transient simulations that the initial conditions will approximate the steady-state head and salinity concentration for a −60 m MSL sea level (which is the average sea level in the Perth region over the past 450 ky). The appropriateness of this initial condition could be assessed by additional modelling that explores the degree of disequilibrium between sea-level (as it varies) and interface position. However, this is also considered outside the scope of the present study.

6. Conclusions

The predicted steady-state salinity distribution in the Perth Basin aquifers is significantly different under sea levels that occurred during the last glacial maximum (i.e., −120 m MSL) than under current sea levels (i.e., 0 m MSL). During lower sea levels of glacial periods, the steady-state interface is predicted to occur close to the furthest offshore extent of the continental shelf. In contrast, under current sea levels and predevelopment heads, the steady-state interface is predicted to occur relatively close to the coast in the Leederville and Yarragadee aquifers. Almost the entire modelled section of the Yarragadee aquifer is predicted to contain groundwater with salinity greater than 20% seawater at a sea level of 0 m MSL. This difference is consistent with the much larger onshore to offshore hydraulic gradient and a shifted shoreline position occurring within each aquifer for the glacial sea-level case compared to the current sea-level case. These results suggest that offshore groundwater in the Perth Basin was emplaced during glacial periods of lower sea levels.

Transient simulations of long-term (i.e., over 20 ky) sea-level variations predict that the interface between seawater and freshwater is likely still moving landward in response to paleo-conditions, although the movement is slow (i.e., a maximum rate of 0.74 m/y was predicted at the base of the Yarragadee aquifer) for the simplified conceptualisation and aquifer parameters used in this study. Transient simulations also predict that onshore groundwater extraction has accelerated seawater intrusion in Perth's offshore aquifers, causing the landward movement of the interface to increase by up to 75% compared to the rate under paleo-conditions alone, at least for the parameters used here. This rate of inland interface movement is relatively slow when compared to a number of well-documented cases of pumping-induced seawater intrusion within onshore aquifers. This is likely, at least in part, to be because the few reported rates of onshore seawater intrusion will be for extreme cases of seawater intrusion.

The Badaminna Fault is predicted to play an important role in determining salinity distribution within Perth's offshore aquifers. Simulations that included the offshore Badaminna Fault indicate that this feature is likely to reduce the offshore extent of fresh groundwater and reduce the rate of inland interface movement associated with paleo-conditions and onshore extraction. Additionally, simulations with the fault produce an offshore fresh groundwater extent that is more in line with measured values than is the case for simulations without the fault. These results highlight a need for further work to unravel the largely unexplored role of offshore faults on the lateral extent and emplacement of offshore fresh groundwater.

The above conclusions are drawn from modelling that used a specified-head inland boundary condition. Additional modelling was carried out using a specified-flux inland boundary condition to explore the influence of the choice of inland boundary condition on steady-state interface position under sea level low-stands, and interface movement under paleo sea-level changes. The specified flux used in the modelling was based on the flux from the specified-head simulation that adopts a sea level of 0 m MSL and a predevelopment inland head. As expected, the steady-state interface was further landward in the specified-flux simulations compared to the specified-head simulations, for the same sea level low-stand. Also, the rate of inland interface movement was less under the specified-flux boundary conditions than the specified-head conditions, as expected. These simulations indicate that under the two "end-member" situations that involve: (a) steeper hydraulic gradients under lower sea levels (as per the specified-head simulations), and (b) the same hydraulic gradient under lower sea level (as per the specified-flux simulations), there is an extensive body of fresh groundwater offshore in the Perth Basin aquifers and the interface is likely still moving landward in response to paleo sea-level change.

This study has highlighted the link between onshore groundwater extraction and offshore fresh groundwater. Offshore fresh groundwater may increase the resilience to salinization of heavily exploited onshore coastal aquifers. However, onshore pumping does induce seawater intrusion within subsea aquifers and, as this study shows for the Perth Basin aquifers, an interface that was already moving landward under paleo-conditions will move landward at a faster rate in response to extraction-induced onshore head declines. Further research is needed to better understand the vulnerability and resilience to seawater intrusion of coastal aquifers that extend offshore using both generic and complex site-specific numerical models that include, for example, three-dimensional flows, sloping stratigraphy, temperature gradients, heterogeneity and faults.

Declarations of interest

None.

Acknowledgements

This work was partly funded by the Perth Region Confined Aquifer Capacity study, Department of Water and Environmental Regulation, Western Australia and Environment Canterbury, New Zealand. Adrian Werner is supported by the Australian Research Council's Future Fellowship scheme, Australia (project number FT150100403). We thank Marc Walther, Alexander Vandenbohede and an anonymous reviewer for their suggestions for improvements to this article.

References

ABS Australian Bureau of Statistics, 2015. Regional Population Growth, Australia, 2013–14. (Accessed 19 September 2016). http://www.abs.gov.au/AUSSTATS/abs@.nsf/Previousproducts/3218.0Main%20Features402013-14?opendocument&tabname=Summary&prodno=3218.0&issue=2013-14&num=&view=.

Amir, N., Kafri, U., Herut, B., Shalev, E., 2013. Numerical simulation of submarine groundwater flow in the coastal aquifer at the Palmahim area, the Mediterranean Coast of Israel. Water Resour. Manag. 27 (11), 4005–4020. https://doi.org/10.1007/s11269-013-0392-2.

Bakker, M., 2006. Analytic solutions for interface flow in combined confined and semi-confined, coastal aquifers. Adv. Water Resour. 29, 417–425. https://doi.org/10.1016/j.advwatres.2005.05.009.

Bakker, M., Miller, A.D., Morgan, L.K., Werner, A.D., 2017. Evaluation of analytic solutions for steady interface flow where the aquifer extends below the sea. J. Hydrol. 551, 660–664. https://doi.org/10.1016/j.jhydrol.2017.04.009.

Barlow, P.M., Reichard, E.G., 2010. Saltwater intrusion in coastal regions of North America. Hydrogeol. J. 18 (1), 247–260. https://doi.org/10.1007/s10040-009-0514-3.

Cai, W.J., Cowan, T., 2006. SAM and regional rainfall in IPCC AR4 models: can anthropogenic forcing account for southwest Western Australian winter rainfall reduction? Geophys. Res. Lett. 33 (24), L24708. https://doi.org/10.1029/2006GL028037.

Cohen, D., Person, M., Wang, P., Gable, C.W., Hutchinson, D., Marksamer, A., Dugan, B., Kooi, H., Groen, K., Lizarralde, D., 2010. Origin and extent of fresh paleowaters on the Atlantic continental shelf, USA. Ground Water 48, 143–158.

Colhoun, E.A., Barrows, T.T., 2011. Chapter 74 – the Glaciation of Australia. In: Jurgen, E., Gibbard, P.L., Hughes, P.D. (Eds.), Developments in Quaternary Science. Elsevier. https://doi.org/10.1016/B978-0-444-53447-7.00074-X.

CSIRO and Bureau of Meteorology, 2015. Climate Change in Australia Information for Australia's Natural Resource Management Regions: Technical Report. CSIRO and Bureau of Meteorology, Australia (Accessed 18 September 2016). http://www.climatechangeinaustralia.gov.au/media/ccia/2.1.5/cms_page_media/168/CCIA_2015_NRM_TechnicalReport_WEB.pdf.

Davidson, W.A., 1995. Hydrogeology and groundwater resources of the Perth Region, Western Australia. West. Australia Geol. Surv. Bull. 142.

Davidson, W.A., Yu, X., 2006. Perth Regional Aquifer Modelling System (PRAMS) Model Development: Hydrogeology and Groundwater Modelling. Hydrogeological Record Series HG 20. Department of Water Government of Western Australia (Accessed 5 July 2017). https://www.water.wa.gov.au/_data/assets/pdf_file/0015/5280/71802.pdf.

Department of Water, 2016a. Water for growth: Urban. Government of Western Australia (Accessed 18 September 2016). http://www.water.wa.gov.au/_data/assets/pdf_file/0016/8521/110200.pdf.

Department of Water, 2016b. Groundwater Chemistry and Isotope Survey, Perth, Western Australia. Aquifer Assessment, Perth Confined Aquifer Capacity Study. Hydrogeological Record Series HR 370. Department of Water, Government of Western Australia.

de Silva, J., 2009. Perth Regional Aquifer Modelling System (PRAMS) Scenario Modelling for the Gnangara Sustainability Strategy, Hydrogeological Record Series, Report No. HG39. Department of Water, Government of Western Australia (Accessed 19 September 2016). http://www.water.wa.gov.au/_data/assets/pdf_file/0012/4323/90782.pdf.

de Silva, J., Wallace-Bell, P., Yesertener, C., Ryan, S., 2013. Perth Regional Aquifer Modelling System (PRAMS) V 3.5 – Conceptual Model, Hydrogeological Report Series, Report No. HR334. Department of Water, Government of Western Australia.

Faure, H., Walter, R.C., Grant, D.R., 2002. The coastal oasis: ice age springs on emerged continental shelves. Glob. Planet. Change 33, 47–56.

Gelhar, L.W., Welty, C., Rehfeldt, K.R., 1992. A critical review of data on field-scale dispersion in aquifers. Water Resour. Res. 28 (7), 1955–1974. https://doi.org/10.1029/92WR00607.

Guo, W., Langevin, C., 2002. User's Guide to SEAWAT: A Computer Program for the Simulation of Three-dimensional Variable-density Ground-water Flow: United States Geological Survey Techniques of Water Resources Investigations, Book 6, Chapter A7. pp. 77. (Accessed 2 May 2015). https://fl.water.usgs.gov/PDF_files/twri_6_A7_guo_langevin.pdf.

Hennig, A., Otto, C., 2005. A Hydrodynamic Characterisation of the Offshore Vlaming Sub-basin. Research Program 1.2 Technologies for Assessing Sites for CO2 Storage. CO2CRC, Canberra, Report No. RPT05-0223.

Houben, G.J., Stoeckl, L., Mariner, K.E., Choudhury, A.S., 2018. The influence of heterogeneity on coastal groundwater flow-physical and numerical modeling of fringing reefs, dykes and structured conductivity fields. Adv. Water Resour. 113, 155–166. https://doi.org/10.1016/j.advwatres.2017.11.024.

Izbicki, J.A., 1996. Seawater Intrusion in a California coastal Aquifer, United States Geological Survey Fact Sheet 125-96. Accessed 6 November 2017. https://pubs.usgs.gov/fs/1996/0125/report.pdf.

Kooi, H., Groen, J., 2001. Offshore continuation of coastal groundwater systems; predictions using sharp-interface approximations and variable-density flow modelling. J. Hydrol. 246, 19–35. https://doi.org/10.1016/S0022-1694(01)00354-7.

Langevin, C.D., Thorne, D., Dausman, A.M., Sukop, M.C., Guo, W., 2008. SEAWAT Version 4: a Computer Program for Simulation of Multi-species Solute and Heat Transport. USGS Techniques and Methods, Book 6, Chapter A22, U.S. Geological Survey.

Leyland, L.A., 2012. Reinterpretation of the Hydrogeology of the Leederville Aquifer, Gnangara Groundwater System, Hydrogeological Record Series HG59. Department of Water, Perth (Accessed 13 January 2017). https://www.water.wa.gov.au/_data/assets/pdf_file/0015/4713/103063.pdf.

Meisler, H., Leahy, P.P., Knobel, L.L., 1984. Effect of Eustatic Sea-level Changes on Saltwater-Freshwater in North Atlantic Coastal Plain, U.S. Geological Survey Water-supply Paper 2255. USGS, Reston, Virginia.

Michael, H.A., Scott, K.C., Koneshloo, M., Yu, X., Khan, M.R., Li, K., 2016. Geologic influence on groundwater salinity drives large seawater circulation through the continental shelf. Geophys. Res. Lett. 43 (20), 10782–10791. https://doi.org/10.1002/2016gl070863.

Mitchell, J.K., Holdgate, G.R., Wallace, M.W., 2007. Pliocene – Pleistocene history of the Gippsland Basin outer shelf and canyon heads, southeast Australia. Aust. J. Earth Sci. 54 (1), 49–64. https://doi.org/10.1080/08120090600981442.

Morgan, L.K., Werner, A.D., 2015. A national inventory of seawater intrusion vulnerability for Australia. J. Hydrol. Reg. Stud. 4, 686–698. https://doi.org/10.1016/j.ejrh.2015.10.005.

MWH, 2011. Perth's Offshore Confined Aquifers Between the Swan River and Guilderton, Prepared by Montgomery Watson Harza (MWH) in Conjunction With the Western Australian Water Corporation. pp. 34.

Passlow, V., Rogis, J., Hancock, A., Hemer, M., Glenn, K., Habib, A., 2005. Final Report, National Marine Sediments Database and Seafloor Characteristics Project. Geoscience Australia, Record 2005/08. (Accessed 29 May 2018). https://www.environment.gov.au/system/files/resources/dad54e03-cb47-4843-a627-

12c7636ce5d2/files/nmb-sediments-report.pdf.
Person, M., Dugan, B., Swenson, J., Urbano, L., Stott, C., Taylor, J., Willet, M., 2003. Pleistocene hydrogeology of the Atlantic continental shelf, New England. Geol. Soc. Am. Bull. 115, 1324–1343. https://doi.org/10.1130/B25285.1.
Post, V.E.A., Groen, J., Kooi, H., Person, M., Ge, S., Edmunds, W.M., 2013. Offshore fresh groundwater reserves as a global phenomenon. Nature 504, 71–78.
Post, V.E.A., Kooi, H., Simmons, C., 2007. Using hydraulic head measurements in variable-density groundwater flow analyses. Groundwater 45 (6), 664–671. https://doi.org/10.1111/j.1745-6584.2007.00339.x.
Siegel, J., Person, M., Dugan, B., Cohen, D., Lizarralde, D., Gable, C., 2014. Influence of late Pleistocene glaciations on the hydrogeology of the continental shelf offshore Massachusetts, USA. Geochem. Geophys. Geosyst. 15 (12), 4651–4670. https://doi.org/10.1002/2014gc005569.
Smith, A.J., Massuel, S., Pollock, D.W., 2011. Geohydrology of the Tamala Limestone Formation in the Perth Region: Origin and Role of Secondary Porosity. CSIRO Report, Australia, pp. 63. https://doi.org/10.4225/08/599dd0fd98a44.
Steffen, W., 2011. The Critical Decade: Western Australia Climate Change Impacts. Climate Commission Secretariat (Department of Industry, Innovation, Climate Change, Science, Research and Tertiary Education), Commonwealth of Australia Accessed 17 September 2016. https://climatecommission.angrygoats.net/topics/western-australia-climate-change-impacts/.
Steffen, W., Hughes, L., 2013. The Critical Decade: Climate Change Science, Response and Risk. Climate Commission Secretariat (Department of Industry, Innovation, Climate Change, Science, Research and Tertiary Education), Commonwealth of Australia Accessed 17 September 2016. https://climatecommission.angrygoats.net/topics/the-critical-decade/.
Voss, C.I., Souza, W.R., 1987. Variable density flow and solute transport simulation of regional aquifers containing a narrow freshwater-saltwater transition zone. Water Resour. Res. 23, 1851–1866. https://doi.org/10.1029/WR023i010p01851.
Water Corporation, 2009. Water Forever: Towards Climate Resilience. (Accessed 18 September 2016). https://www.watercorporation.com.au/-/media/files/about-us/planning-for-the-future/water-forever-50-year-plan.pdf.
Water Corporation, 2011. Water Forever Whatever the Weather. Drought Proofing Perth. (Accessed 11 November 2016). https://www.watercorporation.com.au/-/media/files/about-us/planning-for-the-future/perth-10-year-water-supply-strategy.pdf.
Water Corporation, 2016. Solutions to Perth's Water Supply: Groundwater. (Accessed 18 September 2016). https://www.watercorporation.com.au/water-supply-and-services/solutions-to-perths-water-supply/groundwater.
Werner, A.D., Bakker, M., Post, V.E.A., Vandenbohede, A., Lu, C., Ataie-Ashtiani, B., Simmons, C.T., Barry, D.A., 2013. Seawater intrusion processes, investigation and management: recent advances and future challenges. Adv. Water Resour. 51, 3–26. https://doi.org/10.1016/j.advwatres.2012.03.004.
Werner, A.D., 2017. On the classification of seawater intrusion. J. Hydrol. 551, 619–631. https://doi.org/10.1016/j.jhydrol.2016.12.012.
Werner, A.D., Robinson, N.I., 2018. Revisiting analytical solutions for steady interface flow in subsea aquifers: aquitard salinity effects. Adv. Water Resour. 116, 117–126. https://doi.org/10.1016/j.advwatres.2018.01.002.
Yokoyama, Y., Lambeck, K., De Deckker, P., Johnston, P., Fifield, L.K., 2000. Timing of the last glacial maximum from observed sea-level minima. Nature 406 (6797), 713–716. https://doi.org/10.1038/35021035.
Zheng, C., Bennett, G.D., 2002. Applied Contaminant Transport Modeling, 2nd edition. Wiley Interscience, New York.